

This paper was presented at a colloquium entitled “Physical Cosmology,” organized by a committee chaired by David N. Schramm, held March 27 and 28, 1992, at the National Academy of Sciences, Irvine, CA.

## Preliminary results from the third flight of the Millimeter Anisotropy Experiment (MAX)

M. DEVLIN\*†, D. ALSOP\*†, A. CLAPP\*†, D. COTTINGHAM\*†, M. FISCHER\*†, J. GUNDERSEN\*‡, W. HOLMES\*†, A. LANGE\*†, P. LUBIN\*‡, P. MEINHOLD\*‡, P. RICHARDS\*†, AND G. SMOOT\*†¶

\*The Center for Particle Astrophysics at the University of California, Berkeley, CA 94720; †Department of Physics, The University of California, Berkeley, CA 94720; ‡Department of Physics, The University of California, Santa Barbara, CA 93106; and ¶Lawrence Berkeley Laboratory, Berkeley, CA 94720

**ABSTRACT** Preliminary results from the June 1991 flight of MAX are presented. Simultaneous observations were made in bands centered at 6, 9, and 12 cm<sup>-1</sup> with a bolometric receiver operating at 300 mK. The experimental sensitivities are the highest reported at angular scales of 0.3° to 1.0°. Interstellar dust is observed to have an emissivity  $\propto \nu^{1.4 \pm 0.3}$  and to correlate with the Infrared Astronomical Satellite (IRAS) 100- $\mu$ m map. After removal of emission from interstellar dust, 1.3 hr of integration on a 6° scan yields an upper limit of temperature difference  $\Delta T/T < 2.6 \times 10^{-5}$  at a Gaussian autocorrelation function centered at 0.5°. The experiment and data analysis are described.

### Instrument

The MAX instrument is a 1-m, off-axis balloon-borne, attitude-controlled telescope with a chopping secondary mirror and a multichannel bolometric receiver. The beam size is 0.5° full width at half maximum with a 1.3° peak-to-peak sine-wave chop in the azimuthal direction at 5.8 Hz (1, 2). The chopping secondary and primary mirrors are both underfilled to minimize sidelobe response and spillover. The multichannel receiver simultaneously measures the brightness of a single beam on the sky in three passbands centered at 6, 9, and 12 cm<sup>-1</sup>. Bolometric detectors operating at 300 mK provide high sensitivity at these frequencies. In addition to the three active detectors, there is an identical detector which is optically isolated. This dark detector is used to monitor systematic effects which might produce scan-correlated structure. The instrument is calibrated in flight approximately every hour, using a partially reflecting membrane and a black body. Anisotropy data are obtained by scanning the chopped beam in azimuth to subtract instrumental offsets.

The instrument has flown three times. The first two flights were in 1989 and 1990 (2, 3). The third flight took place on June 5, 1991, at the National Scientific Balloon Facility in Palestine, Texas. Lifted by an 11-million-cubic-foot (310,000 m<sup>3</sup>) balloon, the gondola achieved an altitude of 118,000 feet (36,000 m) for 10.5 hr. The instrument performed as expected. The instrument sensitivity to cosmic microwave background (CMB) anisotropy, determined from in-flight calibrations and noise measurements, was 525, 765, and 32,740  $\mu$ K·s<sup>1/2</sup> in the 6-, 9-, and 12-cm<sup>-1</sup> channels, respectively. The primary role of the 12-cm<sup>-1</sup> channel is to allow for spectral discrimination of interstellar dust emission from the other possible sources.

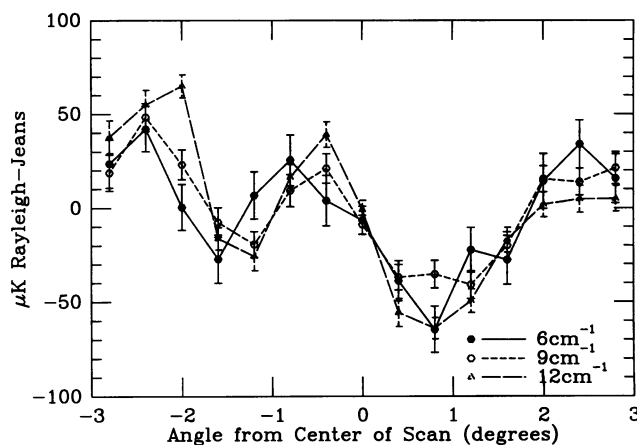


FIG. 1. Data collected near Mu Pegasi from the three optical channels. If a Rayleigh-Jeans source were plotted, it would have the same amplitude in all three channels.

### Analysis

In this flight, a continuous azimuthal scan was performed with a 6° peak-to-peak amplitude and 108-s period. Three CMB observations were performed on different parts of the sky during the flight. The data from the longest integration, obtained near the star Mu Pegasi, will be discussed here. At this position, 45 scans were completed, totaling 1.35 hr of data. After events due to cosmic rays had been removed and a phase-synchronous demodulation of the chopped signal had been performed, the data from each of the four detectors were binned and co-added. The dark channel showed no statistically significant signal during this scan. The data from the 6-, 9-, and 12-cm<sup>-1</sup> channels are shown in Fig. 1. It is apparent that there is a large, spatially correlated signal with an amplitude that increases with frequency. In the 12-cm<sup>-1</sup> channel the signal is approximately 100  $\mu$ K peak-to-peak. To determine what fraction of this signal is due to interstellar dust, a convolution of the beam pattern and scan strategy with the high-resolution Infrared Astronomical Satellite (IRAS) 100- $\mu$ m data was produced. Fig. 2 shows the 12-cm<sup>-1</sup> channel plotted with the IRAS data. The high correlation between the dust-sensitive channel and the IRAS data indicates that anisotropic dust emission dominates the structure in this channel. When the emissivity index  $n$ , where emissivity  $\propto \nu^n$ , between the 12-cm<sup>-1</sup> channel and the IRAS data

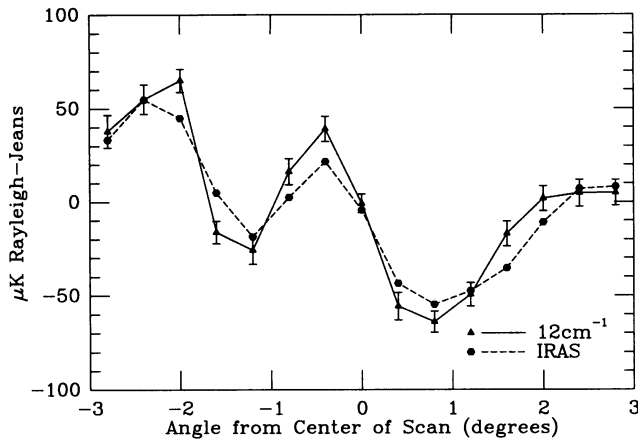


FIG. 2. Data from the 12-cm<sup>-1</sup> channel plotted with the IRAS 100-μm data at the same position on the sky.

is calculated,  $n = 0.9$  for 23 K dust,  $n = 1.2$  for 20 K dust, and  $n = 1.6$  for 18 K dust.

Since it was determined that there is a large contribution to the signal due to dust emission, a method for removing the dust component from the data must be developed so that analysis of CMB anisotropy can be done. Assuming that all of the structure in all three channels is due to a single morphological component of dust and allowing the emissivity to change as a function of frequency, a  $\chi^2$  of  $>45$  with 26 degrees of freedom is obtained. On the basis of this poor fit, a two-signal model is attempted. In this case, the emissivity of the dust is chosen and fixed, and the second component is chosen to have the spectrum of several possible sources of signals in this frequency range. The results shown in Table 1 indicate that all of the two-component models shown have a significantly lower reduced  $\chi^2$  than the single-component model. None of the two-component models listed can be eliminated on the basis of spectral constraints alone. Other models that were tested but did not yield a good fit, such as a 23 K and 5 K dust, are not listed. Because the 12-cm<sup>-1</sup> channel is sensitive to dust, and not the other sources, it determines the shape of the dust signal. The second-component signal for the dust and CMB model is plotted in Fig. 3.

After the second-component signal for the dust and CMB model is obtained, it is possible to set an upper limit on CMB fluctuations, under the assumption that all of the second component is due to CMB fluctuations. Fig. 4 shows the result of this analysis. In addition to the upper limit, the instrument sensitivity is also shown.

**Discussion**

While it is the case that the 95% confidence upper limit shown in Fig. 4 is above the instrument sensitivity, thus implying that a statistically significant has been detected, a 95% confidence lower limit is not quoted. The lower limit is omitted for several reasons. The level of the signal indicates only about a  $2\sigma$  deviation from a straight line. This makes it very difficult to unambiguously eliminate contamination from

Table 1. Results of fitting the data obtained near Mu Pegasi

Model	Emissivity index of dust, $n$ ( $\epsilon \propto \nu^n$ )	$\chi^2/\text{degrees of freedom}$
Dust	Variable	45/26
Dust + CMB	$1.4 \pm 0.3$	16.2/13
Dust + synchrotron	$1.3 \pm 0.3$	17.7/13
Dust + bremsstrahlung	$1.4 \pm 0.3$	16.2/13

The dust used is 23 K.

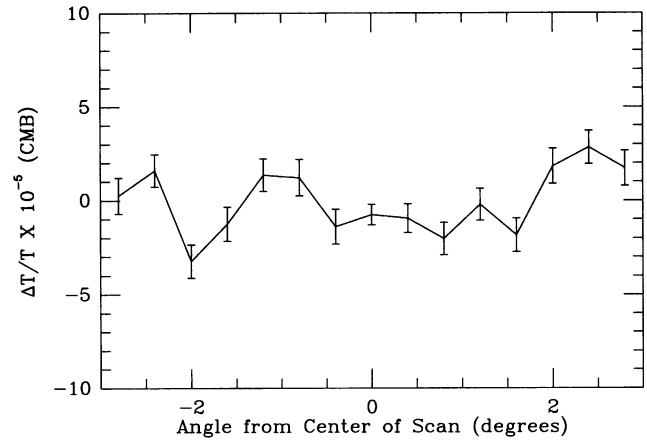


FIG. 3. The CMB component of a dust + CMB model fit to the data collected near Mu Pegasi. The vertical units are 10-ppm changes in the absolute temperature of the CMB.

low-level systematics such as side-lobe contamination. It is also possible that the dust model used in the fitting is oversimplified—i.e., that the morphology of the structure due to dust emission is significantly different at 6 and 9 cm<sup>-1</sup> than at 12 cm<sup>-1</sup>. Synchrotron and bremsstrahlung emission become weak candidates for the origin of the signal when the level of the fluctuations measured at 408 MHz (4) is extrapolated to these frequencies by using standard scaling models. The resulting signals have too small an amplitude.

**Future of MAX**

MAX is evolving to answer the questions posed by each successive flight. It is important to point out that the results described above refer to a region of the sky that is relatively bright in dust. The IRAS 100-μm data indicate that there are portions of the sky that have dust contrast 1/5 to 1/10 that of this region. In the fall of 1992, a 100-mK bolometric receiver is scheduled to be flown which should have 3 to 4 times greater sensitivity than the previous flight. This instrument will achieve a sensitivity of  $\Delta T/T = 3 \times 10^{-6}$  in 1.3 hr of integration. Modified observing strategies of low dust contrast regions will be implemented to test for side-lobe contamination. The addition of a fourth optical channel at 3 cm<sup>-1</sup> will help to eliminate synchrotron and bremsstrahlung as

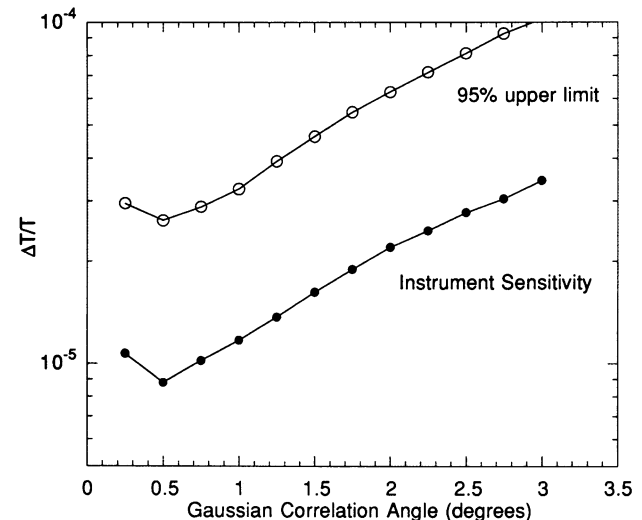


FIG. 4. Limits on CMB anisotropy assuming that all of the second-component signal is due to CMB fluctuations.



sources of signals by using spectral constraints. In conjunction with preparing this receiver, an array receiver is being developed. The array receiver will have 8–12 multifrequency pixels, each with the same sensitivity as the 100-mK receiver. The array receiver will enable sensitive maps to be made of approximately 50 pixels per flight, allowing study of the morphology as well as the spectrum of anisotropic structure.

1. Meinhold, P., Clapp, A., Cottingham, D., Devlin, M., Fischer, M., Gundersen, J., Holmes, W., Lange, A., Lubin, P., Richards, P. & Smoot, G. (1993) *Astrophys. J. Lett.*, in press.
2. Fischer, M. L., Alsop, D. C., Cheng, E. S., Clapp, A. C., Cottingham, D. A., Gundersen, J. O., Koch, T. C., Kreysa, E., Meinhold, P. R., Lange, A. E., Lubin, P. M., Richards, P. L. & Smoot, G. F. (1992) *Astrophys. J.* **388**, 242–252.
3. Alsop, D. C., Cheng, E. S., Clapp, A. C., Cottingham, D. A., Fischer, M. L., Gundersen, J. O., Kreysa, E., Lange, A. E., Lubin, P. M., Meinhold, P. R., Richards, P. L. & Smoot, G. F. (1992) *Astrophys. J.* **395**, 317–325.
4. Haslam, C. G. T., Klein, U., Salter, C. J., Stoffel, H., Wilson, W. E., Cleary, M. N., Cooke, D. J. & Thomasson, P. (1981) *Astron. Astrophys.* **100**, 209–219.